

Comparison Analysis of the Heading Accuracy of GPS, E-compass and Gyroscope

Rosen Miletiev¹, Radostin Kenov², Ivaylo Simeonov³, Emil Iontchev⁴

Abstract – A comparison analysis for heading determination is described that includes the effects of pitch and roll as well as the magnetic properties of the vehicle. Using 3D MEMS magnetic sensor and a linear accelerometer, a low-cost compass system can be realized which accuracy is compared with the GPS and gyroscope data. The proposed system has an integrated Kalman filter for the pitch and roll calculation to build a tilt compensated compass. The heading accuracy is better than the GPS COG data due to the high update rate – up to 75 Hz.

Keywords – heading angle, GPS, e-compass, gyroscope.

I. INTRODUCTION

Navigation is a key ability of mobile systems. The task of navigation can be divided into localization and path planning. Aim of localization is to estimate position and orientation of a mobile system with respect to its environment. The absolute position and heading angle determination of moving objects is necessary for their long term reliable operation. Commonly used heading sensors include difference odometers, gyros and electronic magnetic compasses as well as GNSS receivers [1-4]. The GPS has become the primary source of providing navigation information for most of the present vehicular navigation applications. However, the main disadvantages of GPS receivers towards the course estimation are recognized as a low update rate (usually 1 Hz) and the impossibility to provide continuous navigation solutions in the periods of no signal reception. On the contrary, an INS is a self-contained positioning device that continuously measures three orthogonal linear accelerations and three angular rates to calculate the required position. However, the error of accelerometers will be double integrated and cause position error that accumulate with time.

The current paper discusses the comparison analysis of the heading accuracy of the GPS receiver, MEMS gyroscope and tilt compensated e-compass. The designed heading determination system utilizes three of the above mentioned

sensors, i.e. an electronic compass, a GNSS receiver and a gyro which may work independently. The main subsystem is an electronic compass module. This part of the system allows heading calculation, based on the Earth magnetic field measurements after a calibration procedure implementation. The data of the GNSS receiver, gyroscope and electronic compass module are used to compare the accuracy and the stability towards heading determination. Primary the e-compass heading estimation may be based on the data of the three axis linear accelerometer where the accelerometer readings provide pitch and roll angle information which is used to correct the magnetometer data, but this tilt-compensated e-compass will not operate under freefall or high-g accelerations. This requires a Kalman filter implementation to calculate the proper pitch and roll values according to the gyroscope and accelerometer data.

II. BACKGROUND

The comparison analysis of the heading calculation is accomplished on the basis of the 9DoF inertial system shown at Fig. 1. It consists of 3 axes gyroscope, 3 axes accelerometer and 3 axes magnetometer as a part of 9DoF IMU system and Kalman filter which is integrated into the navigation processor. The roll and pitch angles are established according to the gyroscope and accelerometer data by the Kalman filter and the calculated angles are used in the e-compass to calculate heading on the basis of the tilt compensated compass equations.

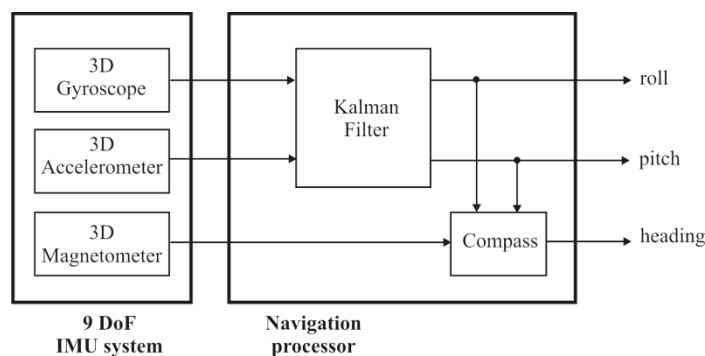


Fig. 1. Block diagram of the heading estimation system

A compass is shown at Fig. 2 with roll (θ) and pitch (ϕ) tilt angles referenced to the right and forward level directions. The X, Y, and Z magnetic readings may be transformed to the horizontal plane (X_h, Y_h) by applying the rotation equations shown in Eq. (1) [5].

$$\begin{aligned} X_h &= X \cdot \cos(\phi) + Y \cdot \sin(\theta) \cdot \sin(\phi) - Z \cdot \cos(\theta) \cdot \sin(\phi) \\ Y_h &= Y \cdot \cos(\theta) + Z \cdot \sin(\theta). \end{aligned} \quad (1)$$

¹Rosen Miletiev is with the Faculty of Telecommunications at Technical University of Sofia, 8 Kl. Ohridski Blvd, Sofia 1000, Bulgaria. E-mail: miletiev@tu-sofia.bg.

²Radostin Kenov is with the Faculty of Telecommunications at Technical University of Sofia, 8 Kl. Ohridski Blvd, Sofia 1000, Bulgaria. E-mail: rkenov@hotmail.com.

³Ivaylo Simeonov is with the Faculty of Computer Systems and Control at Technical University of Sofia, 8 Kl. Ohridski Blvd, Sofia 1000, Bulgaria. E-mail: ivosim@abv.bg.

⁴Emil Iontchev is with the Higher School of Transport "T. Kableskov" 158 Geo Milev Street, Sofia 1574, Bulgaria, E-mail: e_iontchev@yahoo.com.

Heading is defined as the angle in the local horizontal plane measured clockwise from a true North (earth's polar axis) direction. Pitch is defined as the angle between the aircraft's longitudinal axis and the local horizontal plane (positive for nose up). Roll is defined as the angle about the longitudinal axis between the local horizontal plane and the actual flight orientation (positive for right wing down) [6].

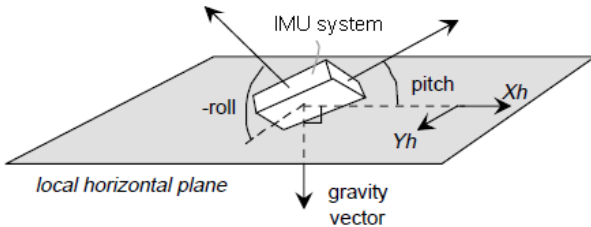


Fig. 2. Definition of the system angles

Heading is defined as the angle in the local horizontal plane measured clockwise from a true North (earth's polar axis) direction. Pitch is defined as the angle between the aircraft's longitudinal axis and the local horizontal plane (positive for nose up). Roll is defined as the angle about the longitudinal axis between the local horizontal plane and the actual flight orientation (positive for right wing down) [6].

Once the magnetic components are found in the horizontal plane, Eq. (1) can be used to determine heading. To account for the arcTan limits, the heading calculations must account for the sign of the Xh and Yh readings as shown below:

$$\begin{aligned} \text{Heading for } (X_h < 0) &= 180 - \arctan(Y_h/X_h) \\ \text{for } (X_h > 0, Y_h < 0) &= -\arctan(Y_h/X_h) \\ \text{for } (X_h > 0, Y_h > 0) &= 360 - \arctan(Y_h/X_h) \\ \text{for } (X_h = 0, Y_h < 0) &= 90 \\ \text{for } (X_h = 0, Y_h > 0) &= 270. \end{aligned} \quad (2)$$

III. COMPASS CALIBRATION

An application of electronic compasses in land vehicles poses serious problems with their installation and calibration. Magnetic disturbances from metal parts of the vehicle and its load, as well as from nearby objects passed by the vehicle may seriously affect the accuracy of measurements. The advantage of compass consists in its bounded errors, not increasing with the time of operation or the distance travelled by the vehicle.

When a two-axis (X,Y) magnetic sensor is rotated in the horizontal plane, the output plot of Xh vs. Yh will form a circle centered at the (0,0) origin. The effect of a magnetic disturbance on the heading is defined as circle distortions. Magnetic distortions may be recognized as hard iron and soft iron effects. The Hard iron distortions arise from permanent magnets on the compass platform. These distortions will remain constant and in a fixed location relative to the compass for all heading orientations therefore these effects add a constant magnitude field component along each axes of the sensor output. Hard and soft iron distortions depend from location to location within the same platform. The compass

has to be mounted permanently to its platform to get a valid calibration. A particular calibration is only valid for that location of the compass.

The calibration procedure is accomplished according to the algorithm, described at [7] which is based on the Merayo technique with a non iterative algorithm for scalar magnetometers calibration [8]. This calibration procedure tries to find the best 3D ellipsoid that fits the data set and returns the parameters of this ellipsoid. The algorithm returns the parameters of this ellipsoid (shape U and center c). The Ellipsoid equation is : $(v-c)^*(U^*U)(v-c) = 1$ with v a rough triaxes magnetometer measurement. The calibrated measurement is given by $w = U^*(v-c)$ [7].

The calibration data are extracted from the total amount of magnetic data for the specific calibration route which is a part of the test track (Fig. 3). The calibration route is chosen on the basis of its semi-circle shape and this route is passed four times to ensure the needed amount of calibration data.

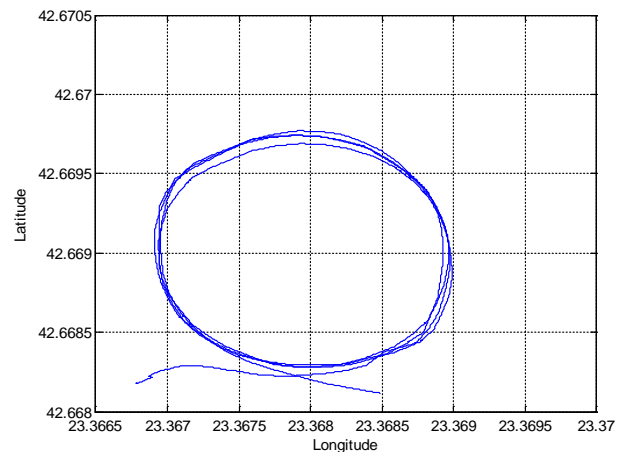


Fig. 3. The calibration route shape

As the calibration procedure is finished the calibrated magnetic data are shown at Fig. 4. The ellipsoid parameters are listed at Table I.

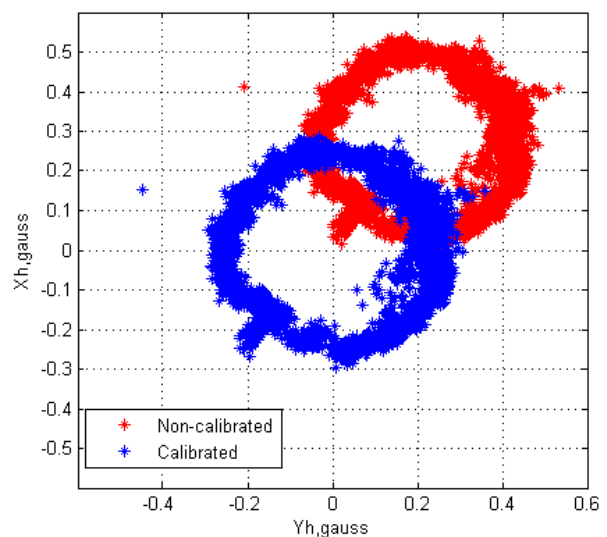


Fig. 4. Xh/Yh diagram before and after calibration

TABLE I
3D ELLIPSOID PARAMETERS

Parameter	Description	Value
a	sub axis (radius) of the X axis of the non-tilt ellipse	0.2362
b	sub axis (radius) of the Y axis of the non-tilt ellipse	0.2295
phi	orientation in radians of the ellipse (tilt)	0.7616
X0	center at the X axis of the non-tilt ellipse	0.0543
Y0	center at the Y axis of the non-tilt ellipse	0.3312
X0_in	center at the X axis of the tilted ellipse	0.2679
Y0_in	center at the Y axis of the tilted ellipse	0.2022
long axis	size of the long axis of the ellipse	0.4723
short axis	size of the short axis of the ellipse	0.4589

IV. HEADING ACCURASY ANALYSIS

The comparison analysis of the heading accuracy is accomplished by the test drive according to the track shown at Fig. 5. This test route also includes the calibration route shown at Figure 3 on the top of the tested one. This route combines a long straight line route and nearly circular calibration route. The heading calculations are made by the GPS receiver, three axes MEMS gyroscope and e-compass, calibrated according to the procedure described at the previous section.

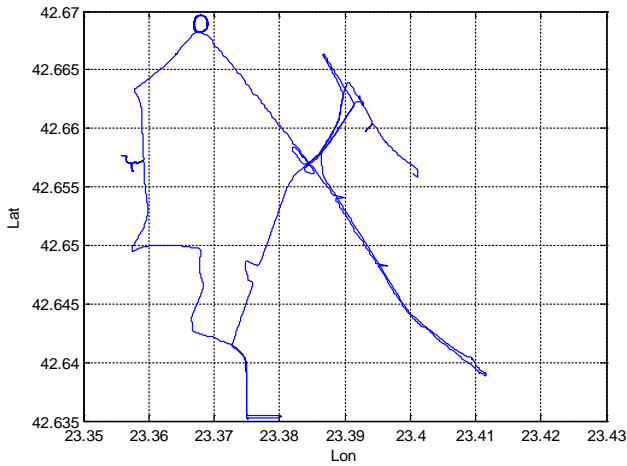


Fig. 5. The test drive track

The comparison of the short-term heading accuracy calculated by the e-compass versus GPS and gyroscope heading data is shown at Figs. 6 and 7 respectively. This comparison analysis is fulfilled on the calibration route as the e-compass is preliminary calibrated and also tilt compensated according to the roll and pitch values on the Kalman filter output. The gyroscope data are obtained after the gyroscope bias compensation according to the last gyroscope bias value

of the stationary object. The gyroscope course is calculated by the numerical integration of the compensated gyroscope data. It is clearly visible that the heading accuracy is very high of the tested navigation subsystems.

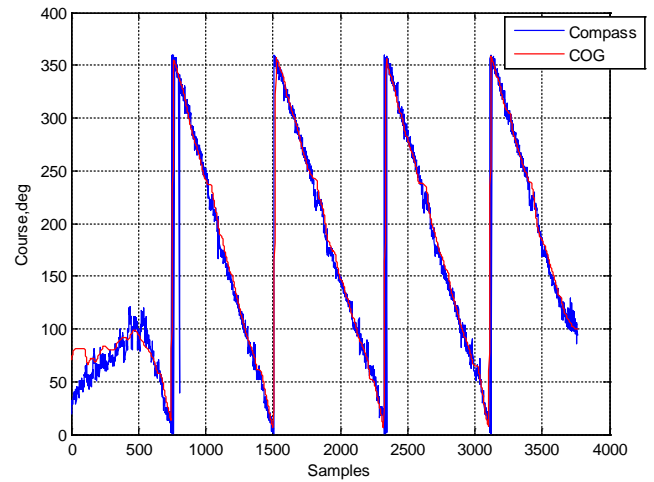


Fig. 6. Short-term heading accuracy (e-compass vs GPS receiver)

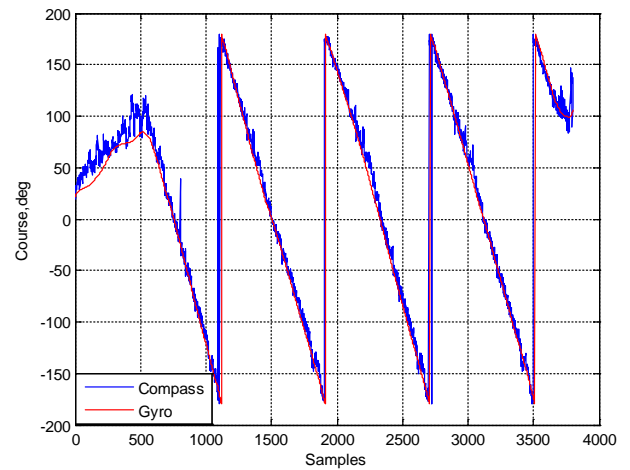


Fig. 7. Short-term heading accuracy (e-compass vs Gyro)

The comparison of the long-term heading accuracy shows slightly different picture. The heading accuracy of the e-compass remains unchanged while the object is non-stationary. Due to the high update rate of the magnetometer (up to 75Hz) the heading accuracy is higher than the GPS receiver which COG (course over ground) value is fixed at the last calculated value (Fig. 8). The long-term test also includes the short-term test shown between sample numbers $2,55 \div 2,6 \cdot 10^5$. Therefore the compass heading has long-term stability, but is noisy and requires an additional signal processing (high-pass filtering, smoothing, etc.).

In the same time the heading accuracy of the gyroscope subsystem is totally violated due to the time-varying gyroscope bias value (Fig. 9). Therefore the gyro has short-term stability but the accuracy is significantly decreased at a time which requires an adaptive gyro bias compensation.

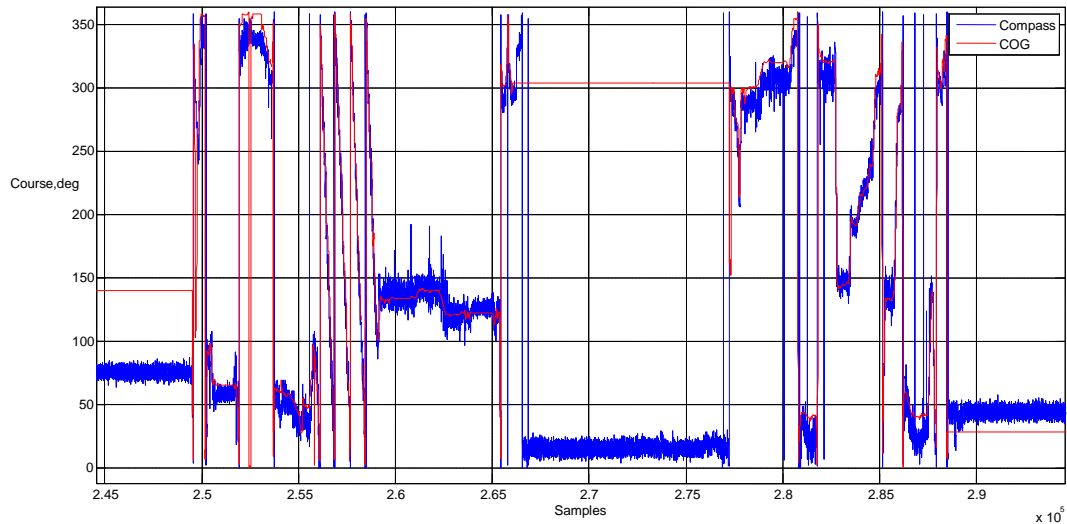


Fig. 8. Long-term heading accuracy of e-compass versus GPS data

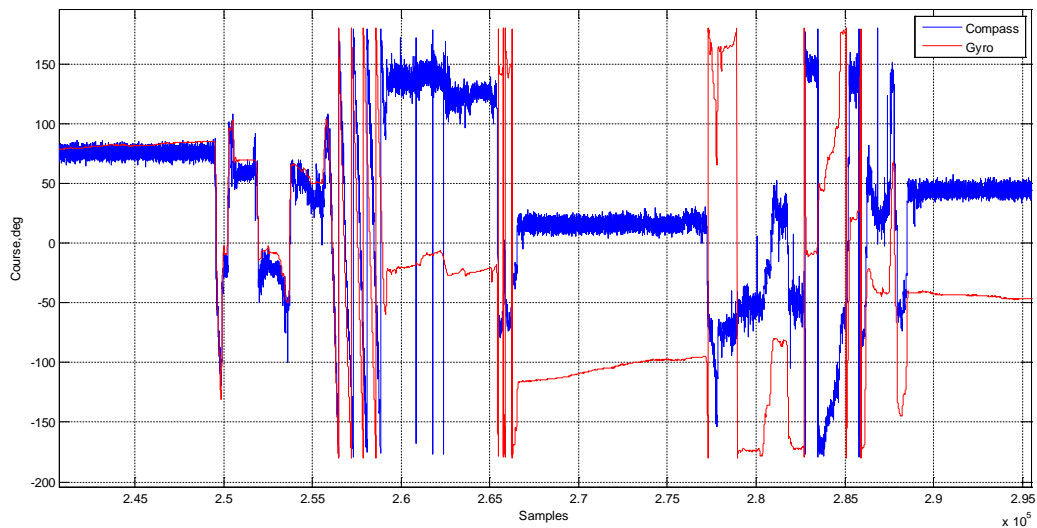


Fig. 9. Long-term heading accuracy of e-compass versus gyro data

V. CONCLUSION

The comparison analysis of the heading accuracy is accomplished using three independent subsystems – GPS receiver, tilt compensated e-compass and low cost gyro. The comparison analysis shows that the e-compass included as a subsystem in the inertial navigation systems may correctly calculate the object course for a long period of time while the gyroscope is distinguished only with a short-term accuracy and the long-term heading accuracy may be achieved only with the adaptive compensation of the bias offset. This compensation is out of the scope of this paper and will be discussed in our future work.

REFERENCES

- [1] M.J. Caruso, Applications of Magnetic Sensors for Low Cost Compass Systems, PLANS, London 2000, p. 177.
- [2] Q. Ladetto, V. Gabaglio, B. Merminod, *Combining Gyroscopes, Magnetic Compass and GPS for Pedestrian Navigation*, KIS, Banff, Canada 2001, p. 205.
- [3] J. Stephen, G. Lachapelle, *J. Navigation* 54, 297 (2001).
- [4] Electronic Tilt Compensation, Application Note AN-00MM-004, Memsic 2008.
- [5] T. Ozyagcilar - Implementing a Tilt-Compensated eCompass using Accelerometer and Magnetometer Sensors, Freescale Semiconductor, Document Number: AN4248, Rev.3, 01/2012.
- [6] M.J. Caruso, Applications of Magnetic Sensors for Low Cost Compass Systems, Honeywell, SSEC.
- [7] A. Barraud, Magnetometers calibration, 03/2009.
- [8] J. Merayo et al. "Scalar calibration of vector magnetometers", *Meas. Sci. Technol.* 11 (2000) 120-132.